Age-Specific Effects on Rat Lung Glutathione and Antioxidant Enzymes after Inhaling Ultrafine Soot

Jackie K. W. Chan[1], Sean D. Kodani[1], Jessie G. Charrier[2], Dexter Morin[3], Patricia C. Edwards[1], Donald S. Anderson[1], Cort Anastasio[2], and Laura S. Van Winkle[1,4]

[1]Center for Health and the Environment; [2]Land Air and Water Resources; [3]Department of Veterinary Medicine: Molecular Biosciences, and [4]Department of Veterinary Medicine: Anatomy, Physiology and Cell Biology, University of California at Davis, Davis, California

Vehicle exhaust is rich in polycyclic aromatic hydrocarbons (PAHs) and is a dominant contributor to urban particulate pollution (PM). Exposure to PM is linked to respiratory and cardiovascular morbidity and mortality in susceptible populations, such as children. PM can contribute to the development and exacerbation of asthma, and this is thought to occur because of the presence of electrophiles in PM or through electrophile generation via the metabolism of PAHs. Glutathione (GSH), an abundant intracellular antioxidant, confers cytoprotection through conjugation of electrophiles and reduction of reactive oxygen species. GSH-dependent phase II detoxifying enzymes glutathione peroxidase and glutathione S-transferase facilitate metabolism and conjugation, respectively. Ambient particulates are highly variable in composition, which complicates systematic study. In response, we have developed a replicable ultrafine premixed flame particle (PFP)-generating system for *in vivo* studies. To determine particle effects in the developing lung, 7–day-old neonatal and adult rats inhaled 22 $\mu g/m^3$ PFP during a single 6-hour exposure. Pulmonary GSH and related phase II detoxifying gene and protein expression were evaluated 2, 24, and 48 hours after exposure. Neonates exhibited significant depletion of GSH despite higher initial baseline levels of GSH. Furthermore, we observed attenuated induction of phase II enzymes (glutamate cysteine ligase, glutathione reductase, glutathione S-transferase, and glutathione peroxidase) in neonates compared with adult rats. We conclude that developing neonates have a limited ability to deviate from their normal developmental pattern that precludes adequate adaptation to environmental pollutants, which results in enhanced cytotoxicity from inhaled PM.

Keywords: glutathione S-transferases; glutathione peroxidase; oxidative stress; lung development; ultrafine particulate matter

CLINICAL RELEVANCE

This study compares how glutathione and glutathione-related enzymes are affected by combustion generated ultrafine particulate matter (PM) between neonatal and adult rats in the lung. Knowing how this important antioxidant pathway is affected upon PM exposure reveals important age-specific differences in antioxidant enzyme expression, which may help explain enhanced susceptibility to PM in young children.

Urban ambient particulate aerosols are an aggregate of small particles, liquid droplets, and vapors that has been linked to respiratory and cardiovascular morbidity and mortality in susceptible populations (1, 2). Young children are especially susceptible to inhaled environmental pollutants. Factors that make children susceptible include enhanced physical and aerobic activities, larger body surface area to volume ratio, higher metabolic rate and minute ventilation, and increased oxygen consumption compared with adult rats (3). Furthermore, the lung continues to grow postnatally while undergoing alveolarization. This occurs on a backdrop of continuous differentiation and maturation of critical cell types in the epithelium (4, 5) that may be disrupted through environmental insults.

Vehicle exhaust from combustion of gasoline, diesel, and other petroleum fuels is a dominant contributor to fine ($PM_{2.5}$) and ultrafine ($PM_{0.1}$) particulates (6) and contains emissions of carbonaceous particles with fused and free polycyclic aromatic hydrocarbons (PAHs). PAH metabolism through phase I xenobiotic metabolism generates electrophilic and reactive metabolites that have been indicated as inducers of pulmonary cytochrome P450 s in diesel exhaust particles (7, 8). Furthermore, ambient PM contains persistent free radicals and reactive oxygen species (ROS) implicated in the generation of cellular oxidative stress (9). Persistent oxidative stress contributes to decreased lung function and increased diagnosis and exacerbation of asthma, bronchitis, and pneumonia in children living in areas of high levels of particulate air pollution (10, 11). Although exposure to $PM_{0.1}$ has been linked to diminished lung development and function in children (12, 13), the underlying biological mechanisms responsible for enhanced susceptibility remain elusive.

Although many nonenzymatic antioxidants are present in the lung, glutathione (GSH) is the most abundant antioxidant, produced in millimolar concentrations in the cell. It is essential for cellular protection through the conjugation of electrophiles and reduction of ROS. GSH is a cofactor for the selenoenzyme glutathione peroxidase (GPX1) and is a cosubstrate in reactions facilitated by glutathione S-transferases (GST). GSH can be replenished through reduction of glutathione disulfide (GSSG) by glutathione reductase (GSR) or through biosynthesis via the γ-glutamyl cycle (14). The γ-glutamyl cycle consists of two ATP-dependent steps, where amino acids L-cysteine, L-glutamic acid, and glycine are combined to form the GSH tripeptide. The first, rate-limiting step combines L-glutamate and cysteine to form γ-glutamylcysteine via the enzyme glutamate cysteine ligase (GCL) before adding glycine to generate GSH. GCL is an oxidant-sensitive heterodimer composed of a catalytic (GCLC)

(*Received in original form March 19, 2012 and in final form September 18, 2012*)

This work was supported by Cellular and Molecular Imaging Core Facility and the inhalation exposure facility at the California National Primate Research Center grant RR00169, by United States Environmental Protection Agency grant RD-83241401–0, by STAR Fellowship Assistance Agreement no. FP-91718101–0 awarded by the USEPA (J.G.C.), by National Institute of Environmental Health Sciences grant P42ES004699, and by a training program in Environmental Health Sciences (grant T32 ES 007059) (J.K.W.C.).

Correspondence and requests for reprints should be addressed to Laura S. Van Winkle, Ph.D., Department of Anatomy, Physiology and Cell Biology, School of Veterinary Medicine., University of California-Davis, Davis, CA 95616-8732. E-mail: lsvanwinkle@ucdavis.edu

This article has an online supplement, which is accessible from this issue's table of contents at www.atsjournals.org

Am J Respir Cell Mol Biol Vol 48, Iss. 1, pp 114–124, Jan 2013

Originally Published in Press as DOI: 10.1165/rcmb.2012-0108OC on October 11, 2012
Internet address: www.atsjournals.org

and a regulatory (GCLM) subunit. Both have been shown to be up-regulated after oxidative stress (15, 16).

Field studies indicate the composition of ambient PM is highly variable and is dependent on the time, day, weather, and location. The variable nature of ambient PM complicates the systematic study of health effects, so we have developed and characterized a premixed flame particle (PFP)-generating system (17, 18) for *in vivo* chamber inhalation exposure studies. Ethylene flame–generated PFPs are 70-nm ultrafine particles rich in PAHs that are also present in the vapor phase. It has previously been shown that, although a quarter of deposited ultrafine particles are cleared by mucoiliary clearance within 24 hours after exposure, a significant fraction of particles are retained within the lungs even after 48 hours (19). In the current study, we exposed male, 7-day-old neonatal pups and 8-week-old young adult rats to a single acute inhalation exposure to PFPs and collected samples at various times up to 48 hours after exposure. We have previously shown that neonates have enhanced susceptibility to PFPs compared with adult rats (18). To further investigate possible mechanisms responsible for the enhanced cytotoxicity, we analyzed GSH levels as well as biosynthesis and conjugating enzymes related to the glutathione pathway (Figure 1). We hypothesized that basal differences and responses between neonates and adult rats would play a role in the enhanced neonatal susceptibility to PFP. The objectives of this study were (*1*) to quantify basal GSH and GSSG levels between adult rats and neonates and their responses after exposure, (*2*) to define the pattern of expression of key GSH resynthesis enzymes after PM oxidative stress, and (*3*) to describe differential responses of conjugating enzymes GPX1 and GSTs.

MATERIALS AND METHODS

Flame and Particle Generation

PFPs were burner generated (17, 18) at a mass concentration of 22.4 ± 5.6 μg/m^3 PFP (mean ± SD) with a mean particle size of 70.6 nm ± 1.5. Particles were high in organic carbon with an lelemental carbon:organic carbon ratio of 0.58.

Animal Exposure Protocol

Eight-weekold male adult rats and newborn postnatal male Sprague Dawley rats with dams (Harlan Laboratories, Indianapolis, IN) were acclimated in filtered air (FA) for 5 to 7 days before use as previously described (17, 18). Animals were necropsied at 2, 24, and 48 hours after cessation of the 6-hour exposure to FA or PFP.

HPLC

Lungs were inflated with a solution of 1% agarose (Sigma Chemical, St. Louis, MO). Airways and surrounding parenchyma were separated by microdissection and prepared for HPLC analysis of GSH and GSSG as described (20), with alterations listed in the online supplement.

RNA Isolation and Real-Time PCR

Microdissected lung compartmental RNA was isolated (21). Gene expression was determined using Taqman probes and primers (Applied Biosystems, Foster City, CA) (21, 22) listed in Table 1. Results were calculated using the comparative-Ct method (23, 24) with hypoxanthine-guanine phosphoribosyltransferase as the reference gene (18, 25). Results are expressed as fold changes relative to filtered animals of the same age unless otherwise stated.

Immunohistochemistry

Lungs were inflated with 37% formaldehyde vapor bubbled under 30 cm hydrostatic pressure for 1 hour and embedded in paraffin within 24 hours (26, 27). Paraffin sections from all groups were stained simultaneously to minimize variability and were immunostained for GSR (Abcam, Cambridge, MA) at 1:500, GPX1 (Abcam) at 1:2,000, and GCL (Neomarkers, Fremont, CA) at 1:300. The concentration of primary antibody was determined through a series of dilutions to optimize for staining density while minimizing background (25, 28).

Western Blotting

Flash-frozen lung tissue was homogenized in RIPA lysis buffer (Santa Cruz Biotechnology, Santa Cruz, CA), and protein concentrations were determined with the Bradford assay (Bio-Rad, Hercules, CA) using BSA as standards. Samples were reduced for SDS-PAGE, and 20 to 40 μg protein per lane was electrophoresed and probed against GPX1, GSR, GCL, and Actin (details are provided in the online supplement). Bands were quantified using ImageJ software (NIH, Bethesda, MD).

Hydrogen Peroxide Assay

Hydrogen peroxide (H_2O_2) production from PFP was measured in triplicate in an *in vitro*, cell-free surrogate lung fluid containing ascorbate, citrate, glutathione, and urate (29). H_2O_2 was quantified using HPLC with fluorescence detection (30). Details are provided in the online supplement.

Statistics

All data are reported as mean ± SEM unless otherwise stated. Statistical outliers were eliminated using the extreme studentized deviate method. Undetected and samples below detection limit were imputed using natural-log regression on order statistics (lnROS) (31, 32). Multivariate ANOVA (MANOVA) was applied against age, compartment, and exposure factors when appropriate. Pairwise comparisons were performed individually using one-way ANOVA followed by Fisher's protected least significant difference *post hoc* analysis using StatView (SAS, Cary, NC). P values of < 0.05 were considered statistically significant.

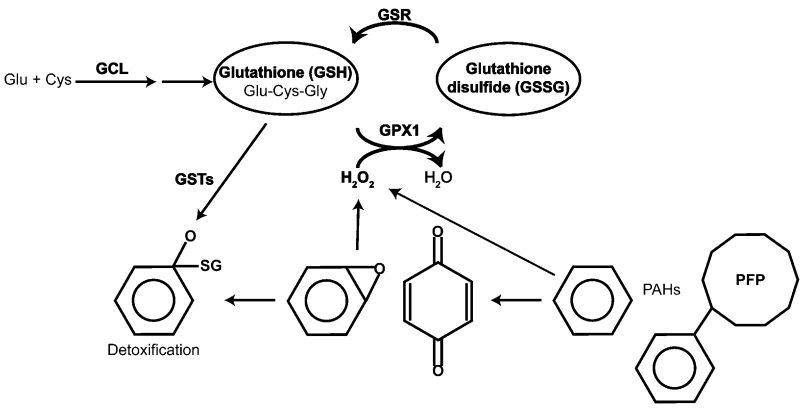

Figure 1. Diagram of glutathione cycle and proposed premixed flame particle (PFP) metabolism indicating endpoints analyzed in this study. PFP directly or indirectly, through the generation of electrophiles, produces hydrogen peroxide and other reactive oxygen species. Glutathione (GSH) conjugates these reactive species directly or through the glutathione S-transferase (GST) enzymes. GSH can be generated through two separate pathways: *de novo* through the γ-glutamyl cycle with glutamate cysteine ligase (GCL) as the rate-limiting enzyme or via reduction of glutathione disulfide through GSR. Bolded portions of these pathways were analyzed in the current study.

TABLE 1. TAQMAN GENE EXPRESSION ASSAY CATALOG NUMBERS

Symbol	Assay ID	Gene Name	NCBI RefSeq
GCLc	Rn00563101_m1	Glutamate-cysteine ligase catalytic subunit	NM_012815.2
GCLm	Rn00568900_m1	Glutamate-cysteine ligase regulatory subunit	NM_017305.2
GPX1	Rn00577994_g1	Glutathione peroxidase	NM_030826.3
GSR	Rn01482159_m1	Glutathione reductase	NM_053906.2
GSTM1	Rn00755117_m1	Glutathione S-transferase Mu-1	NM_017014.1
GSTP1	Rn00561378_gH	Glutathione S-transferase Pi-1	NM_012577.2
GSTT1	Rn00583932_m1	Glutathione S-transferase Theta-1	NM_053293.2
HPRT	Rn01527840_m1	Hypoxanthine-guanine phosphoribosyltransferase	NM_012583.2

RESULTS

GSH and GSSG

We measured levels of the ubiquitous antioxidant GSH and its oxidized dimerized form (Figure 2). We used MANOVA to analyze whether age (neonates versus adult rats), compartment (airway versus parenchyma), or exposure (FA versus PFP2 or PFP24) were contributing factors to measured differences in GSH levels. We collected time-matched FA and PFP samples at 2 and 24 hours after exposure. GSH levels were similar across FA2 and FA24 in neonates and adult rats and were pooled for analysis. GSH levels differed significantly by age ($P = 0.0002$), with 4- to 5-fold higher GSH concentrations in neonates. The MANOVA value for the compartment factor ($P = 0.0074$) signified elevated parenchymal GSH. Neonates had approximately 5 times more GSH in airways and parenchyma compared with adult rats. GSH levels were similar between compartments within each age. After PFP exposure, an abrupt drop in GSH was observed in PFP24 neonates in airway ($P = 0.017$) and parenchymal ($P = 0.0074$) compartments compared with FA controls (Figure 2A). Adult rats showed an opposite response; we observed a time-dependent increase of GSH concentration in the parenchyma that reached significance in PFP24 ($P = 0.036$). Airway GSH levels remained unchanged after exposure (Figure 2B). Multivariate analysis on GSSG concentrations did not convey any significant main effects. Pairwise comparisons revealed significantly higher basal GSSG levels in neonate airways compared with adult rats. A precipitous drop in airway GSSG was observed in neonates after PFP exposure in the PFP24 group, compared with FA controls ($P = 0.032$) and PFP2 ($P = 0.0058$). Neonatal parenchymal GSSG remained unchanged after exposure (Figure 2C). Adult parenchymal GSSG showed a time-dependent increase in response to PFP exposure. Parenchymal GSSG in the PFP24 group was elevated significantly compared with the FA control ($P < 0.0001$) and PFP2 ($P < 0.0001$) groups. Contrary to neonates, airway GSSG was unaffected by PFP exposure (Figure 2D).

Glutamate Cysteine Ligase

To investigate particle effects on GSH regeneration, we analyzed expression of glutamate GCL, the rate-limiting enzyme in GSH biosynthesis (14). We measured mRNA expression levels for the catalytic (GCLC) and regulatory (GCLM) subunits using RT-PCR in the airway and parenchymal lung compartments in 7-day postnatal and adult animals (Figure 3). We used MANOVA to determine whether age, compartment, and exposure (FA versus PFP2, PFP24, or PFP48) factors played a role in GCLC and GCLM expression. We found multiple interactions, with a significant effect of age ($P < 0.0001$); GCL expression was greatest in adults. Furthermore, there was a main effect in compartment ($P < 0.0001$), signifying greater airway expression. A complete table of pairwise comparisons in FA controls showing P values and significant up- or down-regulation is available in the online supplement (*see up and down arrows* in Table E1 in the online supplement). Although GCLM expression remained relatively constant across age and compartments, GCLC expression was 2-fold greater in the airways compared with parenchyma in both ages. Adults generally had a 1.7-fold greater GCLC expression than neonates, with the highest levels in the airways (Figure 3A). In neonates, we observed a transient drop in airway GCLC expression at PFP24 compared with PFP2, whereas parenchymal and GCLM expression remained unchanged after PFP exposure (Figure 3B). In comparison, there were no significant exposure effects for GCLC or GCLM expression in each lung compartment in adult animals (Figure 3C).

GCLC and GCLM protein expression was quantified using Western blotting (Figure 4A). Pairwise comparisons revealed no exposure effects in either subunit in neonates (Figure 4B), but a transient up-regulation in GCLC expression was observed in the adult PFP2 group ($P = 0.048$) compared against FA controls. Adult GCLM expression was also unaffected by PFP exposure (Figure 4C). We performed immunohistochemistry to determine spatial localization of the protein in the lung tissue. We observed intense GCL staining in airway epithelium and parenchyma in PFP2 groups of neonates (Figure 4E) and adult rats (Figure 4I) compared with FA controls. Although neonatal GCL expression reverted to FA distribution and abundance at PFP24 and PFP48 (Figures 4F and 4G), adult GCL expression remained elevated and was localized in the airway epithelium (Figures 4J and 4K).

GSR

Next, we examined the other arm of GSH regeneration: NADPH-mediated reduction of GSSR back to GSH via GSR (Figure 5). Gene expression and MANOVA revealed little difference in GSR expression against age, exposure, and compartment factors. We discovered a single difference: adult airways had significantly greater GSR expression after PFP48 compared with FA controls ($P = 0.0077$). GSR protein expression (Figure 5D) was relatively similar to the RT-PCR results. Although GSR protein abundance was unchanged after PFP exposure (Figure 5E), we saw an almost significant increase in the adult PFP48 group compared against FA controls ($P = 0.06$) (Figure 5F). Immunohistochemical localization of GSR showed mirrored trends from the Western blots. We did not see any GSR protein in FA neonates (Figure 5G). After exposure, the observed transient GSR staining in the bronchiolar epithelium in PFP2 (Figure 5H) returned to FA steady state by PFP24 and PFP48 (Figures 5I and 5J). Adult animals have more abundant basal GSR staining compared with neonates (Figure 5K), which was also enhanced after PFP exposure. Starting at PFP2, we detected robust bronchiolar epithelial staining, which persisted to PFP48 (Figures 5L–5N). Furthermore, several intensely stained cells within the parenchymal tissue could be seen solely in the PFP48 group.

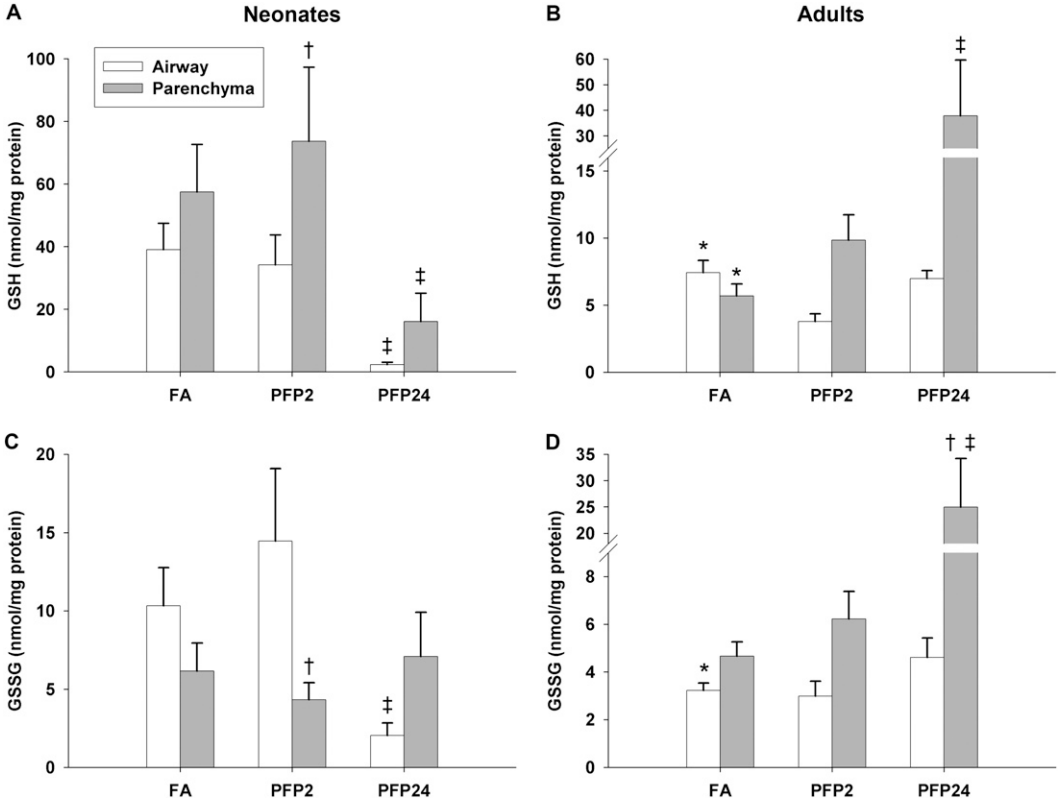

Figure 2. GSH (*A* and *B*) and glutathione disulfide (GSSG) (*C* and *D*) concentrations were measured in microdissected airway (*white bars*) and parenchymal (*gray bars*) tissue compartments using HPLC with electrochemical detection in neonatal (*A* and *C*) and adult (*B* and *D*) rats. Overall, neonates exposed to filtered air (FA) had approximately 5-fold greater GSH in both lung compartments compared with adult rats. After PFP exposure, neonatal GSH levels were significantly depressed in PFP24 compared with FA and PFP2 (*A*). Adult GSH, however, showed an increase in parenchymal GSH in PFP24 (*B*). GSSG levels followed a similar trend. Neonatale airway GSSG was markedly dropped in PFP24 (*C*), whereas adult parenchymal GSSG experienced a time-dependent increase (*D*). Data are plotted as means ± SEM (n = 6–12 rats per group, per compartment). $P < 0.05$ are denoted as follows: *significantly different from neonates in the same compartment, †significantly different from airways in the same exposure and age, and ‡significantly different from FA in the same compartment and age.

GPX1

GPX1 decreases reactive hydroperoxides using glutathione as a cosubstrate (33), making it a suitable candidate to analyze the effects of ROS on glutathione-dependent antioxidant enzymes (Figure 6). Using RT-PCR and performing MANOVA against age, exposure, and compartment factors, we detected significant age ($P < 0.0001$), exposure ($P = 0.0031$), and compartment ($P = 0.0007$) effects. Adults had a significantly higher GPX1 expression, which was increased by PFP exposure and was greater in parenchyma compared with in airways. To determine the specific differences, we applied pairwise comparisons against individual groups. Although GPX1 expression was similar between the airway and parenchyma compartments in neonates, adult parenchymal GPX1 expression was significantly greater than adult airways ($P = 0.035$) and neonatal parenchyma ($P = 0.016$) (Figure 6A). After PFP exposure, neonatal GPX1 expression was significantly down-regulated in the PFP48 group in airway and parenchyma compartments compared with the PFP24 group (Figure 6B). A divergent trend was observed in adult rats. Compared with FA controls, we detected significant GPX1 up-regulation in the parenchyma in PFP24 as well as in airways and parenchyma in the PFP48 groups (Figure 6C). Because GPX1 is responsible for reducing hydroperoxides, we measured the rate of H_2O_2 production *in vitro* in a cell-free surrogate lung fluid. We observed substantially more H_2O_2 in the filters containing PFP compared with filter blank controls (Figure 6D). Additionally, we found that PFP particles generate a similar amount of H_2O_2 compared with ambient particulates collected from Fresno, California on a mass-normalized basis (*see* Figure E1 in the online supplement). Next, we analyzed GPX1 protein expression (Figure 6E) to correlate with our previous results. Generally, GPX1 protein is consistent with the mRNA expression data. Although GPX1 abundance was largely unchanged in the neonates (Figure 6F), we found a significant time-dependent increase in adults, where PFP24 ($P = 0.045$) and PFP48 ($P = 0.023$) groups had significantly elevated GPX1 levels compared with FA controls (Figure 6G). Immunohistochemistry localized GPX1 protein to airway epithelium and parenchyma of neonates and adult rats in FA controls, but neonates exhibited a lower overall abundance (Figures 6H and 6L). After PFP exposure, GPX1 remained unchanged in neonates (Figures 6I–6K). In adult rats, PFP induced GPX1 throughout the lung tissue. Staining was darker in all lung compartments; intensely positive staining was observed in bronchiolar epithelium (Figures 6M–6O, *arrows*) regardless of the time after exposure.

GST

We evaluated mRNA expression of the μ (GSTM1), π (GSTP1), and θ (GSTT1) isoforms in the GST family (Figure 7), which catalyze the conjugation of glutathione to electrophilic substrates as a contributor to phase II xenobiotic biotransformation (34). We applied MANOVA against age, compartment, and gene (GSTM1 versus GSTP1 versus GSTT1) factors on FA controls and found significant effects ($P < 0.0001$) in all three main factors (age, compartment, and gene). Pairwise comparisons among GSTs in FA controls are presented in Table E2. Under basal conditions, GSTM1 is expressed 4- to 5-fold higher in airways compared with parenchyma; these findings were consistent between adult rats ($P < 0.0001$) and neonates ($P = 0.006$). Similarly, GSTM1 is 3- to 4-fold higher in adults across compartments, with GSTM1 maximally expressed in adult airways. GSTP1 was the most abundant GST among the three isoforms comparing between ages with the exception in adult airways, where GSTM1 was most abundant. Adult rats had significantly greater GSTP1 expression in airway ($P = 0.021$)

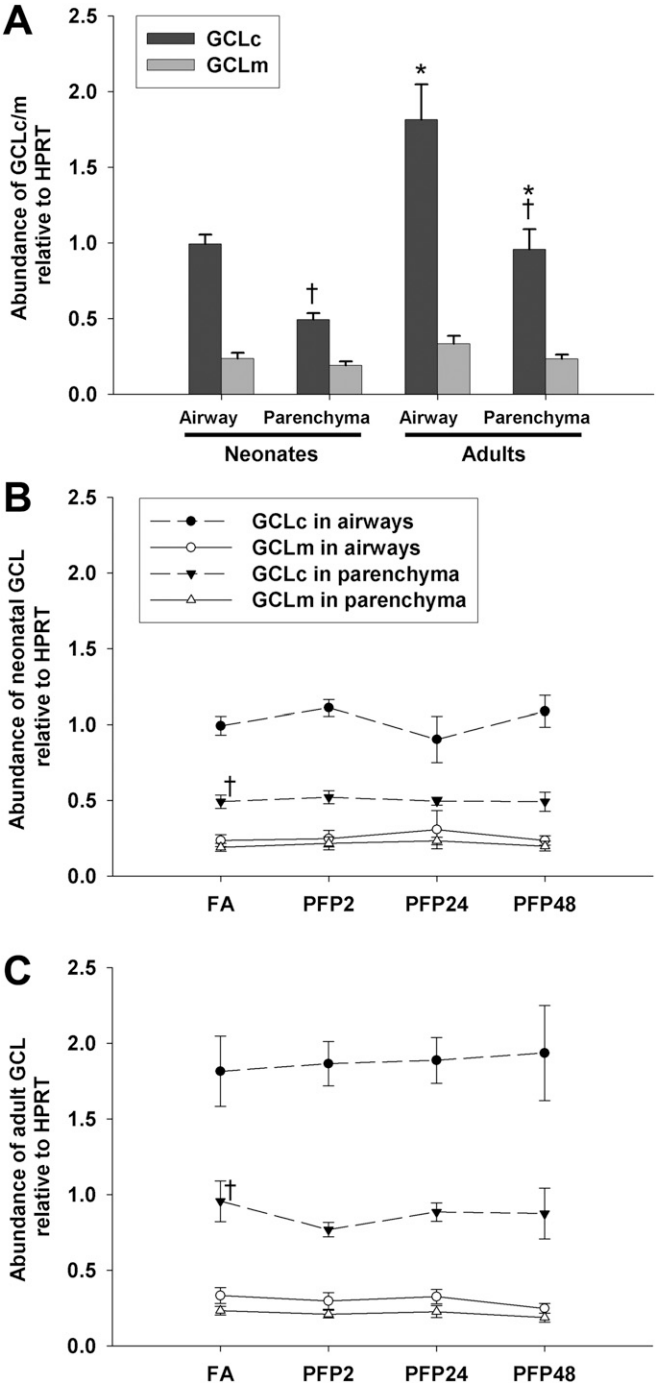

Figure 3. GCLc and GCLm gene expression. RT-PCR expression in airway and parenchyma compartments in neonates and adult rats exposed to PFPs. Basal GCLc was consistently expressed in higher abundance than GCLm, and its highest expression was seen in adult airways (*A*). After PFP exposure, a transient drop in neonatal airway GCLc expression was observed in PFP24 compared with PFP2 (*B*). No treatment effects were detected in adult animals (*C*). Data are plotted as means ± SEM ($n = 5$–7 rats per group, per compartment, per gene). $P < 0.05$ are denoted as follows: *significantly different from neonates in the same compartment, and †significantly different from airways in the same age. PFP2, PFP24, and PFP48 refer to PFP exposure for 4, 24, and 48 hours, respectively.

and parenchyma ($P = 0.016$) compared with neonates, but there were no differences observed between compartments in both age groups. GSTT1 was the least abundant GST isoform but was expressed at levels 2-fold higher in adults than neonates and in the airways than in the parenchyma (Figure 7A). After PFP exposure, GSTM1 expression was significantly elevated in PFP48 adult airways compared with all other exposure time points. Besides a transient increase in neonatal airway PFP2 compared with PFP48, no other age or compartment had significant exposure-related effects (Figure 7B). GSTP1 expression revealed a similar pattern; adult airway expression in PFP48 was significantly greater than all other exposures. However, a transient decrease in GSTP was observed in adult parenchyma in the PFP2 group ($P = 0.049$) that recovered at later time points. Neonatal expression did not differ from FA controls after PFP exposure, but the PFP24 and PFP48 groups were depressed compared against PFP2 in the parenchyma (Figure 7C). Finally, GSTT1 expression was down-regulated in adult PFP24 parenchyma ($P = 0.029$) compared with adult FA controls. No other age or compartment had significantly changed from their respective FA controls (Figure 7D).

DISCUSSION

In the current study, we used site-specific approaches to define GSH and GSSG concentrations as well as expression patterns for a number of antioxidant gene and proteins to identify the underlying cause of enhanced susceptibility in neonatal versus adult rats. To determine how conducting airways and alveoli separately respond to PFP exposure, airways were microdissected from alveolar parenchyma to evaluate compartment-specific responses. We have previously reported that neonates are more susceptible to inhaled PFPs than adults based on elevated LDH leakage and ethidium homodimer-1 staining (18), which has correlated well with the literature on neonatal susceptibility to particulate matter (35, 36). Moreover, we have shown that subchronic exposure to PFPs during this period of development causes decrements in airway growth that are not recovered upon reaching adulthood (17). In other exposure models, inhalation of ultrafine particulates increases airway resistance and decreases compliance (37), suggesting impaired lung function.

We have built upon our previous work by analyzing components of the phase II detoxification pathway, namely GSH-related protective responses. We measured levels of the ubiquitous antioxidant GSH, the GSH biosynthetic enzyme GCL, the GSH regeneration enzyme GSR, the GSH selenoenzyme GPX1, and several isoforms of GST conjugation enzymes. In a majority of these measures, we have noted that neonates remained essentially unchanged after exposure, in striking contrast to an overall up-regulation of the aforementioned antioxidants observed in adults after inhalation of particles. We demonstrated a unique failure of antioxidant proteins in 7-day postnatal rats to respond to an acute, single 6-hour inhalation exposure to an atmosphere containing flame-generated ultrafine particles. This response differed markedly from the effective up-regulation of these antioxidant responses in adult rats.

PFP is an ethylene flame–generated ultrafine carbonaceous soot. It is rich with attached and free PAHs and closely resembles diesel exhaust with a low elemental carbon:organic carbon ratio of 0.58. Methylated biphenyls and substituted naphthalenes are the dominant organic species measured, but larger PAHs, such as fluorene, phenanthrene, pyrene, and benzopyrenes, were also detected in subnanogram quantities (18). Our data revealed that these particles are potent hydrogen peroxide producers and are similar in their peroxide-generating capability to ambient particles collected in Fresno, California. Furthermore, the PFP chamber particle concentration ([9.4 ± 0.5] × 10^4 particles/cm^3) was similar to values reported 30 m downwind from a major highway in Los Angeles, California

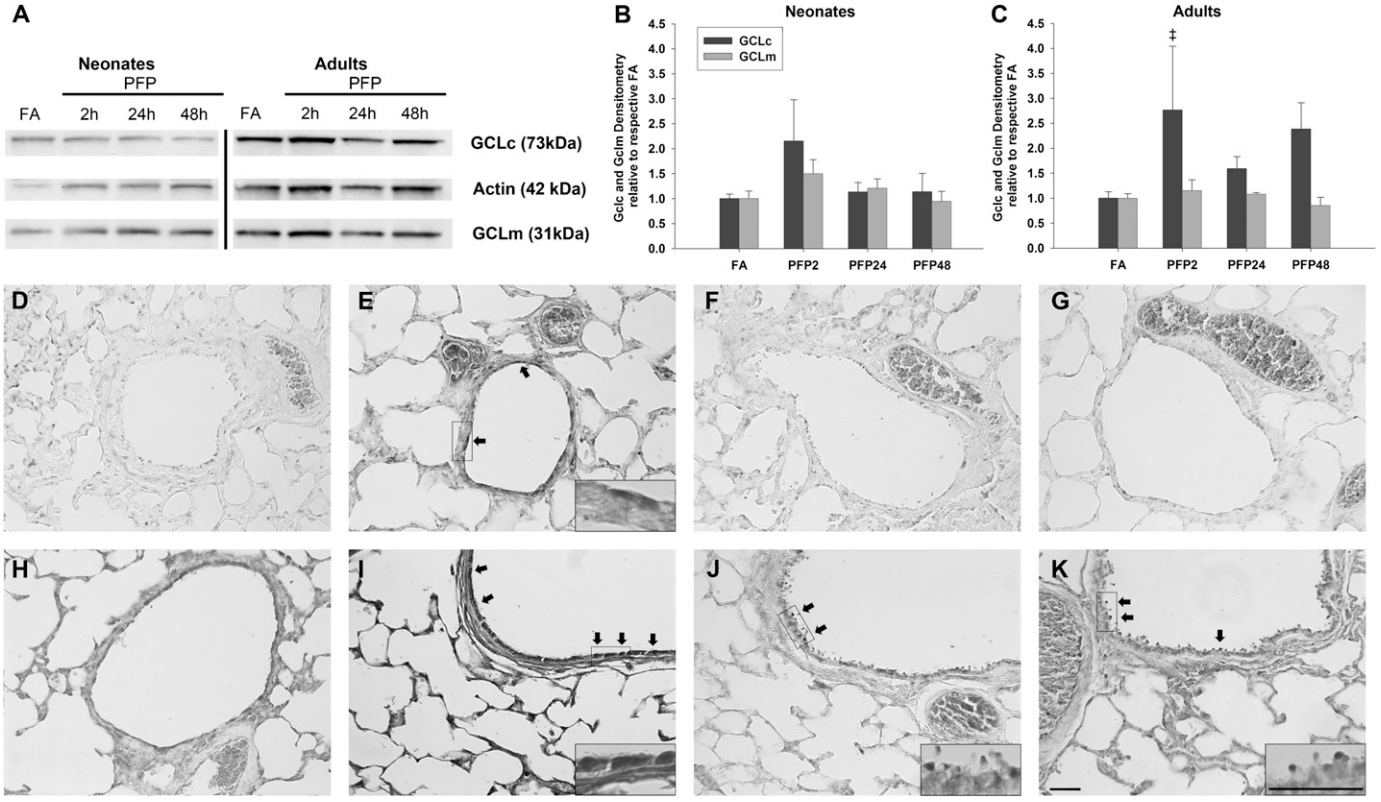

Figure 4. GCLc and GCLm protein analysis through Western blotting and immunohistochemistry. Representative GCLc and GCLm Western blots with actin loading control (*A*). GCLc/m Western blots were quantified: while neonatal GCLc/m expression remained unchanged after exposure (*B*), a significant up-regulation in GCLc was detected in PFP2 adult rats compared against FA controls (*C*). Data are plotted as means ± SEM (n = 6 rats per group). $P < 0.05$ is denoted as follows: ‡significantly different from FA in the same age. GCL immunohistochemical images in neonatal (*D–G*) and adult (*H–K*) rats reared in FA (*D* and *H*) and exposed to PFP: PFP2 (*E* and *I*), PFP24 (*F* and *J*), and PFP48 (*G* and *K*). Intense GCL staining was observed in adult and neonatale PFP2. In contrast to neonates, staining in adult PFP48 was continually up-regulated. High magnification inserts highlight GCL-positive cells in treated groups. *Scale bars* for *D–K* (shown in *K*) are 50 μm.

($\sim 5.0 \times 10^4$ particles/cm^3; 65-nm particles) (38). Our chamber dose (22.4 μg/m^3) is well below the 2006 United States Environmental Protection Agency revised 24-hour average National Ambient Air Quality Standards for $PM_{2.5}$ of 35 μg/m^3, highlighting the importance of using supplementary measurements in addition to PM mass to determine ultrafine particulate contributions to aerosol mass. Our current study shows that neonates respond very differently than adult rats to environmentally relevant levels of fine PM.

Although many antioxidants are present in the rat lung, including a variety of vitamins and ascorbic and uric acids, we limited our analysis to the most ubiquitous antioxidant GSH. We found that neonatal GSH levels were several-fold greater than in adult rats regardless of compartment. This is expected due to initial adaptation to a hyperoxic environment at birth. GSH depletion via buthionine sulfoximine in newborn rats has been shown to be lethal due to the accumulation of endogenous ROS generated from mitochondrial metabolism that induces oxidative stress and injury (39). Although GSH and GSSG results are highly variable among published studies using a variety of methods, our data fall within the ranges (0.54–15.2 nmol/mg protein GSH and 0.069–7.66 nmol/mg protein GSSG) reported previously in control rat lung homogenates (40–42). Our findings are in accordance with previously published data using lung microdissection approaches coupled with HPLC electrochemical detection and fluorescence methods in the rat lung that yielded 4.4 to 9.1 nmol/mg protein airway GSH and 10.26 to 10.6 nmol/mg protein parenchymal GSH (43, 44). After PFP exposure, we observed disparate trends between the two age groups. Adult GSH and GSSG concentrations were elevated 24 hours after exposure solely in the parenchymal compartment. Our findings are in accordance with data reported by Al-Humadi and colleagues, who showed elevated levels of GSH in alveolar macrophages from adult Sprague Dawley rats intratracheally instilled with diesel exhaust particles (45). However, neonatal levels of GSH and GSSG were depressed in the airways. Differences in GSH and GSSG levels between lung compartments and their differential responses to PFP exposure highlights the heterogeneity of the lung, where specific cell populations exist in distinct microenvironments. GSH depletion has been linked with epithelial cytotoxicity, where decrements below a certain threshold cause irreversible injury (46, 47). This correlates well with the compartment-specific cytotoxicity we found in our previous study (18). Additionally, the GSH:GSSG ratio, typically considered an indicator of oxidative stress, was significantly diminished in neonates after exposure but remained unchanged in adult rats. The declining trends in GSH and GSSG after PFP exposure in neonates suggests a failure to up-regulate or regenerate glutathione pools in very young animals.

We analyzed mRNA and protein expression of several glutathione-dependent enzymes: GCL, GSR, GPX1, and several isoforms of GST. These antioxidant enzymes are regulated by the nuclear factor erythroid-derived inducer 2 transcription factor under the antioxidant response element and are activated after exposure to oxidant stressors such as particulate matter (48).

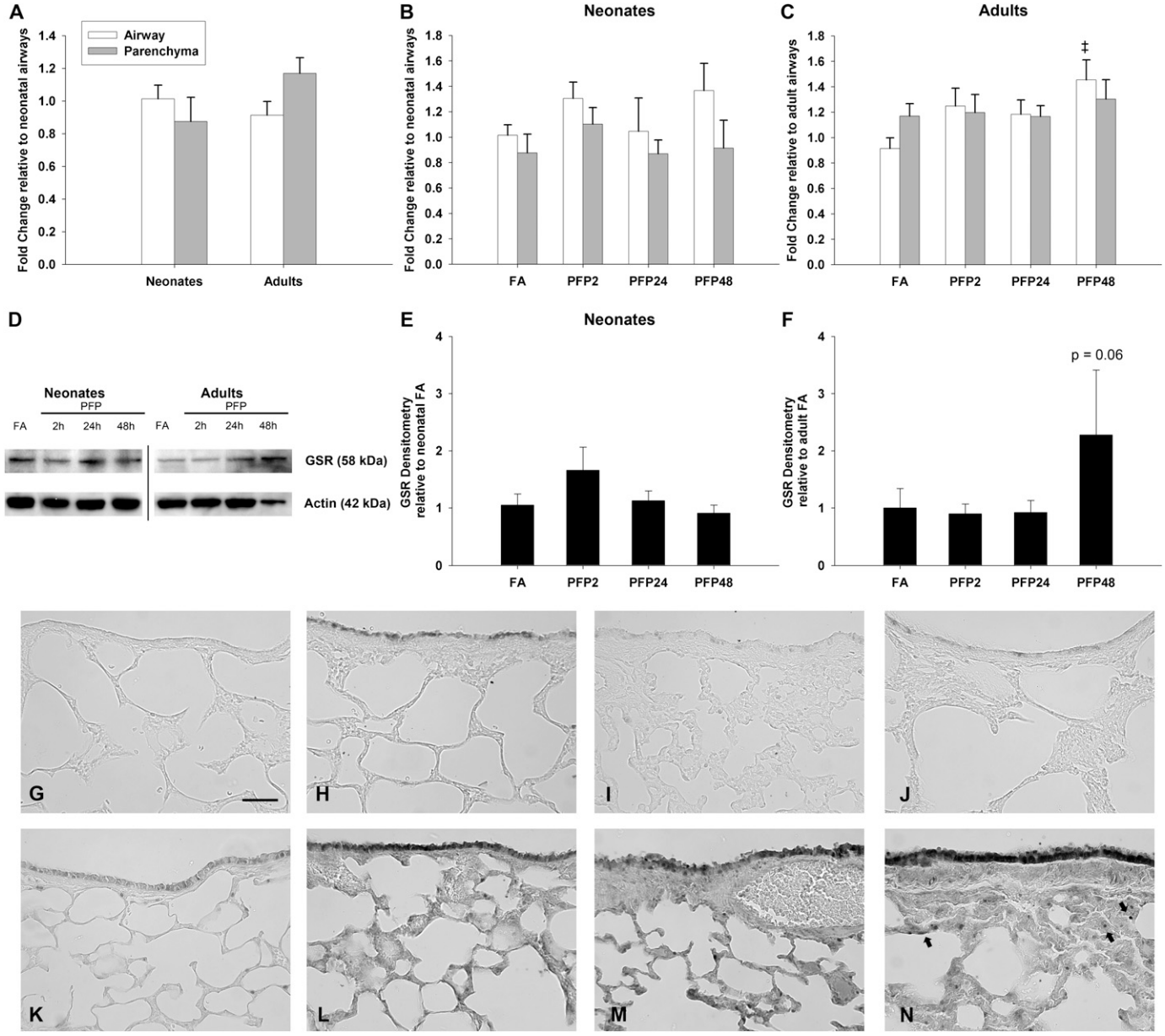

Figure 5. GSR gene and protein expression. Basal GSR gene expression was similar between age and compartments (*A*). No exposure-related gene expression differences were observed in neonates after PFP exposure (*B*). In adult rats exposed to PFPs, a time-dependent increase of GSR gene expression was observed 48 hours after exposure (*C*). Data are plotted as means ± SEM ($n = 6$ rats per group, per compartment). $P < 0.05$ is denoted as follows: ‡significantly different from FA in the same compartment and age. A representative blot of GSR protein with actin as a loading control (*D*). Quantification of GSR Western blots revealed no exposure-related effects in neonates (*E*). In adult animals, there was a strong but insignificant trend 48 hours after PFP exposure (*F*). Protein data are mean ± SEM ($n = 5$ or 6 rats per group). Spatial immunohistochemical localization of GSR in neonatal (*G–J*) and adult (*K–N*) of FA controls (*G* and *K*), PFP2 (*H* and *L*), PFP24 (*I* and *M*), and PFP48 (*J* and *N*) groups. A transient up-regulation was seen in neonatal airways in PFP2, whereas adult animals had continual induction of GSR until PFP48. At PFP48, densely stained cells were observed in the parenchyma (denoted by *arrows*). *Scale bar* for *G–N* (shown in *G*) is 50 μm.

To quantify the potential for GSH regeneration, we evaluated the GCLC and GCLM subunits along with GSR mRNA transcript and protein expression levels. Although basal compartmental and age differences were apparent between the catalytic and regulatory subunits, there were no exposure effects in GCLC/M expression. Our data contrast with published reports demonstrating GCLC/M mRNA up-regulation after ultrafine particulate exposure (49–51). A possible explanation for the disparity may be due to different exposure conditions. Our exposure concentrations were substantially lower (22.4 $\mu g/m^3$ for a single 6-h PFP exposure), compared with these past studies, which used higher doses and longer exposure durations (4-d exposure to 5.0 mg/m^3 ultrafine butadiene-generated soot [49], 8-wk exposure to 100 $\mu g/m^3$ diesel exhaust particulates [50], or 10 wk of reaerosolized ultrafine ambient particulates [51] in mice). Although we did not detect exposure effects in GCLC/M mRNA expression, GCLC protein was elevated after exposure, and this finding is similar to results recently published by Zhang and colleagues, who presented similar GCLC up-regulation results in 3-month-old "young adult" mice after chronic ambient ultrafine particulate (<200 nm) exposure (51). A similar trend is seen with GSR mRNA and protein expression. Although we

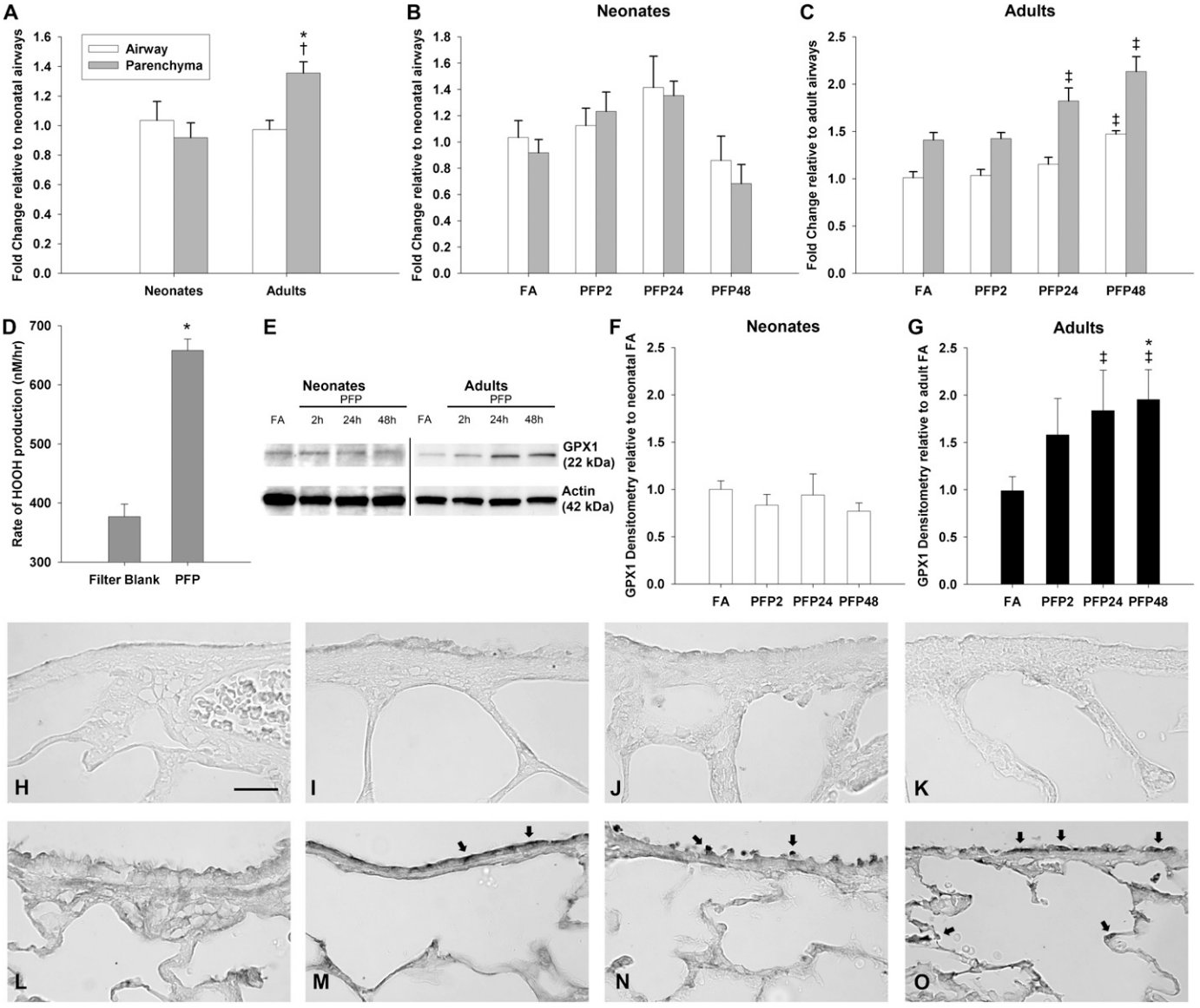

Figure 6. GPX1 gene and protein expression. GPX1 gene expression was greatest in the adult parenchyma; all other age and compartments had similar expression levels (*A*). A significant reduction in GPX1 expression was observed in the PFP48 neonates compared with PFP24 in airways and parenchyma (*B*). Contrary to neonates, GPX1 was up-regulated in adult rats. Parenchymal expression was significantly higher in the PFP24 and PFP48 groups compared with FA controls and with the PFP2 group. Airway expression was significantly higher only in the PFP48 group (*C*). Data are plotted as means ± SEM ($n = 6$ rats per group, per compartment). $P < 0.05$ is denoted as follows: *significantly different from neonates in the same compartment, †significantly different from airways in the same age, and ‡significantly different from FA in the same compartment and age. The rate of H_2O_2 production from PFP was significantly greater than from filter blanks (*D*). Data are plotted as means ± SD ($n = 3$). $P < 0.05$ is denoted as follows: *significantly different from filter blank. GPX1 protein was quantified using Western blotting; a representative blot with actin-loading control is shown (*E*). Quantification of GPX1 Western blots revealed no exposure-related effects in neonates (*F*) nut revealed a time-dependent increase in GPX1 expression in adults after PFP exposure (*G*). Protein data are presented as mean ± SEM (n = 5 or 6 rats per group). $P < 0.05$ is denoted as follows: ‡significantly different compared with FA controls. Spatial expression of GPX1 in neonatal (*H–K*) and adult rats (*L–O*) and of FA controls (*H* and *L*) and PFP2- (*I* and *M*), PFP24- (*J* and *N*), and PFP48- (*K* and *O*) exposed groups. GPX1 induction in adults was seen in airway epithelium and parenchyma. *Arrows* identify intensely stained bronchiolar epithelium present at all time points after PFP exposure. *Scale bar* for *H–O* (shown in *N*) is 50 μm.

did not observe any exposure-related mRNA or protein changes in the neonates, we saw significant increases in adult airway mRNA expression and a strong trend in protein expression in the PFP48 group. These data are similar to previously published data showing enhanced GSR activity in alveolar macrophages of rats intratracheally instilled with diesel exhaust particles (45). The inability of neonates to up-regulate this rate-limiting enzyme, in addition to GSH depletion, may lead to the loss of cellular homeostasis, where ROS generation overwhelms antioxidant defenses, resulting in oxidative stress. This may partially explain why the neonatal rats are more susceptible to an acute PM exposure compared with adult rats.

Cellular GPX1 is a phase II enzyme that confers cytoprotection through metabolism of H_2O_2 and organic peroxides (present endogenously and produced from deposited particulates) that cause protein and lipid peroxidation, generating oxidative stress. Superoxide anion, present in diesel exhaust particulate extracts (52), is a substrate for superoxide dismutase, which converts superoxide into H_2O_2 for GPX1 metabolism. GPX1 is a potent, selenium-dependent antioxidant that consumes GSH

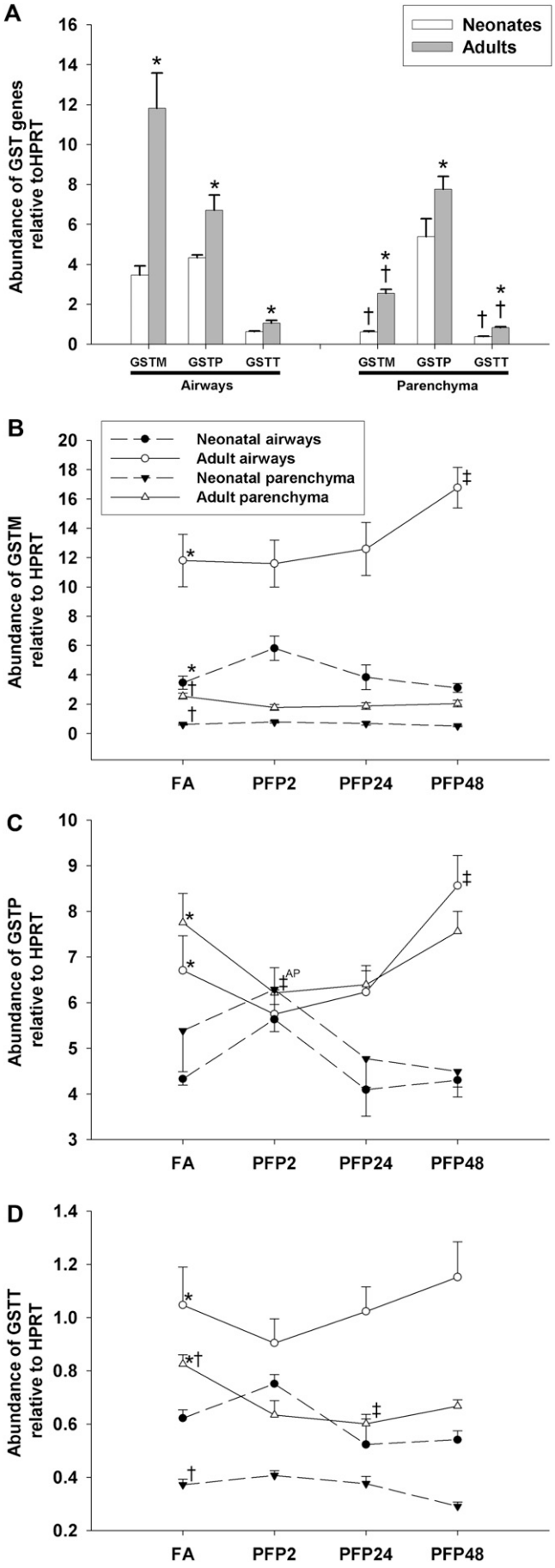

Figure 7. Expression of glutathione S-transferase isoforms (GSTM = SGT μ isoform; GSTP = GST π isoform; and GSTT = GST τ isoform). GSTM had widely variable compartmental and age expression, whereas GSTP had age-specific differences. GSTT was the least abundant isoform but is expressed higher in adults airways (*A*). GSTM expression was significantly up-regulated in adult airways in the PFP48 group compared with all other exposure time points (*B*). GSTP expression was similar: adult airways in the PFP48 group were also significantly elevated against FA controls and exposure groups. A transient drop in adult parenchyma was observed in PFP2 compared with FA controls (*C*). GSTT expression was temporarily down-regulated in adult parenchyma in PFP24 (*D*). Data are plotted as means ± SEM ($n = 5$–7 rats per group, per compartment, per gene). $P < 0.05$ are denoted as follows: *significantly different from neonates in the same compartment, †significantly different from airways in the same age and gene, and ‡significantly different from FA in the same compartment and age. To reduce confusion among comparisons between groups, superscript AP denotes comparison against adult parenchyma.

to reduce these oxidants to preserve cellular homeostasis (33, 53). In the current study, we showed that PFP particles actively generate H_2O_2 in a cell-free surrogate lung fluid and observed time-dependent elevation of GPX1 mRNA and protein expression after exposure in adult animals. Our results are in agreement with previous work that demonstrated GPX1 elevation in adult rats 24 hours after a week-long exposure to cigarette smoke (54). However, in comparison to adult animals, neonates did not reveal the same pattern, and gene transcription and protein expression remained unchanged after inhaling PFPs. The inability to respond could increase neonatal vulnerability to PFP by increasing the burden of intracellular H_2O_2, especially because GPX1 activity is lowest at 6 to 16 days of age (55).

GSTs are a family of phase II detoxification enzymes that catalyze GSH conjugation with electrophilic compounds (34). We focused on the μ (GSTM1), π (GSTP1), and θ (GSTT1) isoforms. These isoforms have significance in antioxidant defense; previous clinical studies have shown adverse allergic responses after inhalation of environmental pollutants in polymorphic or null cohorts (56, 57). GSTM1 and GSTP1 expression was significantly up-regulated only in adult airways at 48 hours after PFP exposure, again highlighting the importance of evaluating compartment-specific effects. Our results are in accordance with previously published data showing specific GSTM1 and GSTP1 induction in airways after treatment with nuclear factor erythroid-derived inducer 2 (3)-tert-butyl-4-hydroxyanisole (58). The failure of neonates to mirror adult responses is concerning because it indicates an inability to up-regulate these protective molecules in the face of a relevant environmental provocation. Children with the GSTM1 null allele or GSTT1 deficiency have increased risk of developing asthma and exacerbation of asthma symptoms, such as wheezing or shortness of breath, after environmental tobacco smoke exposure (59). Furthermore, GSTP1 is critical in the deactivation of cytochrome P450 metabolically activated PAHs present in PFPs. GSTP1 knockout mice are shown to have increased DNA adducts and decreased GSH conjugates after PAH treatment (60). Although GST proteins are detectable by immunochemical methods at 7 days of age, GST–mediated 1-chloro-2, 4-dinitrobenzene conjugation activity is seen only 20% of adults (61). This further highlights the importance of GSTs in the defense against oxidant stressors in the developing lung. The inability to adequately up-regulate key antioxidant enzymes reduces the ability to detoxify electrophilic compounds present on or in ultrafine particles, which may enhance cytotoxicity and increase susceptibility in neonates, who are already at a disadvantage due to the postnatal maturation of this enzymatic activity.

This study shows that a short-term, low-dose inhalation exposure to an environmentally relevant level of combustion-derived ultrafine particles causes up-regulation of glutathione and glutathione-related enzymes in the adult rat. We hypothesize that failure to up-regulate key enzymes is due to a limited availability to deviate from a normal developmental pattern of expression in the postnatal animal. Our data strongly support the notion that the appropriate age group, in our case 7-day-old neonates, be used when evaluating the potential effect of an environmental pollutant on susceptible populations such as young children. We have shown that neonates suffered a precipitous drop in GSH concentrations after PFP inhalation that was not regenerated by GCL or GSR. Furthermore, phase II enzymes such as GSTs and GPX1 remained unchanged after exposure, possibly as a result of the lack of GSH as a reducing substrate, which potentially enhances cytotoxicity in neonates. We conclude that, compared with mature adult rats, the developing lung fails at up-regulating key GSH regeneration and antioxidant enzymes to adequately adapt to ultrafine particulate exposure. The downstream effects may result in enhanced cellular injury and oxidative stress compared with adult rats exposed to the same dose.

Author disclosures are available with the text of this article at www.atsjournals.org.

Acknowledgments: The authors thank Brian Tarkington, Ashley Cooper, Louise Olson, Judy Shimizu, Aamir Abid, and Christopher Wallis for their skilled technical assistance during exposures, sample collection, and processing; Jonathan Rutherford for his expertise in drawing vector graphics; and Dr. Alan Buckpitt for reading and editing this manuscript.

References

1. Dockery DW. Health effects of particulate air pollution. *Ann Epidemiol* 2009;19:257–263.
2. Mills NL, Donaldson K, Hadoke PW, Boon NA, MacNee W, Cassee FR, Sandstrom T, Blomberg A, Newby DE. Adverse cardiovascular effects of air pollution. *Nat Clin Pract Cardiovasc Med* 2009;6:36–44.
3. Bearer CF. How are children different from adults. *Environ Health Perspect* 1995;103:7–12.
4. Finkelstein JN, Johnston CJ. Enhanced sensitivity of the postnatal lung to environmental insults and oxidant stress. *Pediatrics* 2004;113(Suppl) 1092–1096.
5. Langston C. Normal and abnormal structural development of the human lung. *Prog Clin Biol Res* 1983;140:75–91.
6. Pey J, Querol X, Alastuey A, Rodriguez S, Putaud JP, Van Dingenen R. Source apportionment of urban fine and ultra-fine particle number concentration in a western Mediterranean city. *Atmos Environ* 2009; 43:4407–4415.
7. Rengasamy A, Barger MW, Kane E, Ma JK, Castranova V, Ma JY. Diesel exhaust particle-induced alterations of pulmonary phase I and phase II enzymes of rats. *J Toxicol Environ Health A* 2003;66:153–167.
8. Baulig A, Garlatti M, Bonvallot V, Marchand A, Barouki R, Marano F, Baeza-Squiban A. Involvement of reactive oxygen species in the metabolic pathways triggered by diesel exhaust particles in human airway epithelial cells. *Am J Physiol Lung Cell Mol Physiol* 2003;285: L671–L679.
9. Dellinger B, Pryor WA, Cueto R, Squadrito GL, Hegde V, Deutsch WA. Role of free radicals in the toxicity of airborne fine particulate matter. *Chem Res Toxicol* 2001;14:1371–1377.
10. Brunekreef B, Janssen NA, de Hartog J, Harssema H, Knape M, van Vliet P. Air pollution from truck traffic and lung function in children living near motorways. *Epidemiology* 1997;8:298–303.
11. Norris G, Young Pong SN, Koenig JQ, Larson TV, Sheppard L, Stout JW. An association between fine particles and asthma emergency department visits for children in seattle. *Environ Health Perspect* 1999;107:489–493.
12. Ibald-Mulli A, Wichmann HE, Kreyling W, Peters A. Epidemiological evidence on health effects of ultrafine particles. *J Aerosol Med* 2002; 15:189–201.
13. Wichmann HE, Peters A. Epidemiological evidence of the effects of ultrafine particle exposure. *Philos T Roy Soc A* 1775;2000:2751–2768.
14. Meister A. Glutathione, metabolism and function via the gamma-glutamyl cycle. *Life Sci* 1974;15:177–190.
15. Krzywanski DM, Dickinson DA, Iles KE, Wigley AF, Franklin CC, Liu RM, Kavanagh TJ, Forman HJ. Variable regulation of glutamate cysteine ligase subunit proteins affects glutathione biosynthesis in response to oxidative stress. *Arch Biochem Biophys* 2004;423:116–125.
16. Sutherland KM, Edwards PC, Combs TJ, Van Winkle LS. Sex differences in the development of airway epithelial tolerance to naphthalene. *Am J Physiol Lung Cell Mol Physiol* 2012;302:L68–L81.
17. Lee D, Wallis C, Wexler AS, Schelegle ES, Van Winkle LS, Plopper CG, Fanucchi MV, Kumfer B, Kennedy IM, Chan JK. Small particles disrupt postnatal airway development. *J Appl Physiol* 2010;109:1115–1124.
18. Chan JK, Fanucchi MV, Anderson DS, Abid AD, Wallis CD, Dickinson DA, Kumfer BM, Kennedy IM, Wexler AS, Van Winkle LS. Susceptibility to inhaled flame-generated ultrafine soot in neonatal and adult rat lungs. *Toxicol Sci* 2011;124:472–486.
19. Moller W, Felten K, Sommerer K, Scheuch G, Meyer G, Meyer P, Haussinger K, Kreyling WG. Deposition, retention, and translocation of ultrafine particles from the central airways and lung periphery. *Am J Respir Crit Care Med* 2008;177:426–432.
20. Lakritz J, Plopper CG, Buckpitt AR. Validated high-performance liquid chromatography-electrochemical method for determination of glutathione and glutathione disulfide in small tissue samples. *Anal Biochem* 1997;247:63–68.
21. Baker GL, Shultz MA, Fanucchi MV, Morin DM, Buckpitt AR, Plopper CG. Assessing gene expression in lung subcompartments utilizing *in situ* RNA preservation. *Toxicol Sci* 2004;77:135–141.
22. Stelck RL, Baker GL, Sutherland KM, Van Winkle LS. Estrous cycle alters naphthalene metabolism in female mouse airways. *Drug Metab Dispos* 2005;33:1597–1602.
23. Livak KJ, Schmittgen TD. Analysis of relative gene expression data using real-time quantitative PCR and the 2(-delta delta C(t)) method. *Methods* 2001;25:402–408.
24. Schmittgen TD, Livak KJ. Analyzing real-time PCR data by the comparative c(t) method. *Nat Protoc* 2008;3:1101–1108.
25. Van Winkle LS, Chan JK, Anderson DS, Kumfer BM, Kennedy IM, Wexler AS, Wallis C, Abid AD, Sutherland KM, Fanucchi MV. Age specific responses to acute inhalation of diffusion flame soot particles: cellular injury and the airway antioxidant response. *Inhal Toxicol* 2010;22:70–83.
26. Wilson HH, Chauhan J, Kerry PJ, Evans JG. Ethanol vapour-fixation of rat lung for immunocytochemistry investigations. *J Immunol Methods* 2001;247:187–190.
27. Hammond TG, Mobbs M. Lung oedema–microscopic detection. *J Appl Toxicol* 1984;4:219–221.
28. Van Winkle LS, Isaac JM, Plopper CG. Repair of naphthalene-injured microdissected airways *in vitro*. *Am J Respir Cell Mol Biol* 1996;15:1–8.
29. Charrier JG, Anastasio C. Impacts of antioxidants on hydroxyl radical production from individual and mixed transition metals in a surrogate lung fluid. *Atmos Environ* 2011;45:7555–7562.
30. Kok GL, McLaren SE, Staffelbach TA. HPLC determination of atmospheric organic hydroperoxides. *J Atmos Ocean Technol* 1995;12:282–289.
31. Helsel DR. More than obvious: better methods for interpreting nondetect data. *Environ Sci Technol* 2005;39:419a–423a.
32. Shumway RH, Azari RS, Kayhanian M. Statistical approaches to estimating mean water quality concentrations with detection limits. *Environ Sci Technol* 2002;36:3345–3353.
33. Arthur JR. The glutathione peroxidases. *Cell Mol Life Sci* 2000;57: 1825–1835.
34. Armstrong RN. Glutathione S-transferases: reaction mechanism, structure, and function. *Chem Res Toxicol* 1991;4:131–140.
35. Zhong CY, Zhou YM, Smith KR, Kennedy IM, Chen CY, Aust AE, Pinkerton KE. Oxidative injury in the lungs of neonatal rats following short-term exposure to ultrafine iron and soot particles. *J Toxicol Environ Health A* 2010;73:837–847.
36. Pinkerton KE, Zhou Y, Zhong C, Smith KR, Teague SV, Kennedy IM, Menache MG. Mechanisms of particulate matter toxicity in neonatal

and young adult rat lungs. *Res Rep Health Eff Inst* 2008;135:3–41, discussion 43–52.
37. Balakrishna S, Saravia J, Thevenot P, Ahlert T, Lominiki S, Dellinger B, Cormier SA. Environmentally persistent free radicals induce airway hyperresponsiveness in neonatal rat lungs. *Part Fibre Toxicol* 2011; 8:11.
38. Zhu Y, Hinds WC, Kim S, Sioutas C. Concentration and size distribution of ultrafine particles near a major highway. *J Air Waste Manag Assoc* 2002;52:1032–1042.
39. Martensson J, Jain A, Stole E, Frayer W, Auld PA, Meister A. Inhibition of glutathione synthesis in the newborn rat: a model for endogenously produced oxidative stress. *Proc Natl Acad Sci USA* 1991;88:9360–9364.
40. Scott RB, Reddy KS, Husain K, Schlorff EC, Rybak LP, Somani SM. Dose response of ethanol on antioxidant defense system of liver, lung, and kidney in rat. *Pathophysiology* 2000;7:25–32.
41. Perez R, Lopez M, Barja de Quiroga G. Aging and lung antioxidant enzymes, glutathione, and lipid peroxidation in the rat. *Free Radic Biol Med* 1991;10:35–39.
42. Jenkinson SG, Spence TH Jr, Lawrence RA, Hill KE, Duncan CA, Johnson KH. Rat lung glutathione release: response to oxidative stress and selenium deficiency. *J Appl Physiol* 1987;62:55–60.
43. Buckpitt A, Chang AM, Weir A, Van Winkle L, Duan X, Philpot R, Plopper C. Relationship of cytochrome P450 activity to clara cell cytotoxicity: IV. Metabolism of naphthalene and naphthalene oxide in microdissected airways from mice, rats, and hamsters. *Mol Pharmacol* 1995;47:74–81.
44. Duan X, Buckpitt AR, Pinkerton KE, Ji C, Plopper CG. Ozone-induced alterations in glutathione in lung subcompartments of rats and monkeys. *Am J Respir Cell Mol Biol* 1996;14:70–75.
45. Al-Humadi NH, Siegel PD, Lewis DM, Barger MW, Ma JY, Weissman DN, Ma JK. Alteration of intracellular cysteine and glutathione levels in alveolar macrophages and lymphocytes by diesel exhaust particle exposure. *Environ Health Perspect* 2002;110:349–353.
46. Plopper CG, Van Winkle LS, Fanucchi MV, Malburg SR, Nishio SJ, Chang A, Buckpitt AR. Early events in naphthalene-induced acute clara cell toxicity: II. Comparison of glutathione depletion and histopathology by airway location. *Am J Respir Cell Mol Biol* 2001;24: 272–281.
47. Phimister AJ, Lee MG, Morin D, Buckpitt AR, Plopper CG. Glutathione depletion is a major determinant of inhaled naphthalene respiratory toxicity and naphthalene metabolism in mice. *Toxicol Sci* 2004; 82:268–278.
48. Li N, Nel AE. Role of the NRF2-mediated signaling pathway as a negative regulator of inflammation: implications for the impact of particulate pollutants on asthma. *Antioxid Redox Signal* 2006;8:88–98.
49. Rouse RL, Murphy G, Boudreaux MJ, Paulsen DB, Penn AL. Soot nanoparticles promote biotransformation, oxidative stress, and inflammation in murine lungs. *Am J Respir Cell Mol Biol* 2008;39:198–207.
50. Li YJ, Takizawa H, Azuma A, Kohyama T, Yamauchi Y, Takahashi S, Yamamoto M, Kawada T, Kudoh S, Sugawara I. Disruption of NRF2 enhances susceptibility to airway inflammatory responses induced by low-dose diesel exhaust particles in mice. *Clin Immunol* 2008;128:366–373.
51. Zhang H, Liu H, Davies KJ, Sioutas C, Finch CE, Morgan TE, Forman HJ. Nrf2-regulated phase ii enzymes are induced by chronic ambient nanoparticle exposure in young mice with age-related impairments. *Free Radic Biol Med* 2012;52:2038–2046.
52. Kumagai Y, Arimoto T, Shinyashiki M, Shimojo N, Nakai Y, Yoshikawa T, Sagai M. Generation of reactive oxygen species during interaction of diesel exhaust particle components with NADPH-Cytochrome p450 reductase and involvement of the bioactivation in the DNA damage. *Free Radic Biol Med* 1997;22:479–487.
53. Michiels C, Raes M, Toussaint O, Remacle J. Importance of Se-glutathione peroxidase, catalase, and Cu/Zn-sod for cell-survival against oxidative stress. *Free Radic Biol Med* 1994;17:235–248.
54. Gilks CB, Price K, Wright JL, Churg A. Antioxidant gene expression in rat lung after exposure to cigarette smoke. *Am J Pathol* 1998;152:269–278.
55. Fujii T, Endo T, Fujii J, Taniguchi N. Differential expression of glutathione reductase and cytosolic glutathione peroxidase, GPX1, in developing rat lungs and kidneys. *Free Radic Res* 2002;36:1041–1049.
56. Strange RC, Spiteri MA, Ramachandran S, Fryer AA. Glutathione-s-transferase family of enzymes. *Mutat Res* 2001;482:21–26.
57. Gilliland FD, Li YF, Saxon A, Diaz-Sanchez D. Effect of glutathione-s-transferase M1 and P1 genotypes on xenobiotic enhancement of allergic responses: randomised, placebo-controlled crossover study. *Lancet* 2004;363:119–125.
58. Forkert PG, D'Costa D, El-Mestrah M. Expression and inducibility of alpha, pi, and mu glutathione S-transferase protein and mRna in murine lung. *Am J Respir Cell Mol Biol* 1999;20:143–152.
59. Kabesch M, Hoefler C, Carr D, Leupold W, Weiland SK, von Mutius E. Glutathione S transferase deficiency and passive smoking increase childhood asthma. *Thorax* 2004;59:569–573.
60. Ritchie KJ, Henderson CJ, Wang XJ, Vassieva O, Carrie D, Farmer PB, Gaskell M, Park K, Wolf CR. Glutathione transferase Pi plays a critical role in the development of lung carcinogenesis following exposure to tobacco-related carcinogens and urethane. *Cancer Res* 2007;67:9248–9257.
61. Fanucchi MV, Buckpitt AR, Murphy ME, Storms DH, Hammock BD, Plopper CG. Development of phase II xenobiotic metabolizing enzymes in differentiating murine clara cells. *Toxicol Appl Pharmacol* 2000;168:253–267.